HyCal Reconstruction Fine Tuning and Transition Region Performance Measured During Calibration Run

PrimEx Note #83

D. Romanov, I. Larin, A. Gasparian, L. Gan, M. Khandaker, M. Kubantsev

2009 – 2010 & 2017

Abstract

To perform high precision measurement of energy and direction of neutral pions in the PRIMEX experiment, extensive study of resolution function of the HyCal calorimeter was performed using data obtained during dedicated runs with the tagged photon beam. The calorimeter was installed on the moving platform, which allowed irradiating each counter to measure its response. The beam scanned the surface of the detector with "snake" pattern. The detector was calibrated with existing 5x5 reconstruction algorithm after the run and results were reported in [1] and used in the thesis [2]. The purpose of this note is to describe details of the further work, which has been done for the fine reconstruction tuning and study of the reconstruction peculiarities at the transition region.

This note was written based on PrimEx-I run data, which were taken in 2004. We want to mention here, that for PrimEx-II run the island reconstruction algorithm [3] has been added as an option in addition to the 5x5algorithm used for PrimEx-I and in this work. Another progress has been made in the calorimeter timing: HyCal modules have been aligned on trigger time. Hit time delay dependence on energy has been extracted from the data. Time resolution between two hits in HyCal has been obtained and this information has been successfully used to reject accidental background.

1. Position Reconstruction

As a zero approximation of cluster coordinate, we can take a center of gravity of an electromagnetic shower, which is the simplest estimation method:

$$x = \sum x_i \, w_i \qquad (1.1),$$

where x_i - coordinate of the center of i^{th} module and the weight w_i can be taken as a fraction of the shower energy deposited in i^{th} module to the total energy: $w_i = E_i / \sum E_i$.

It is well known that such a method gives unbiased estimation only in the center and at the edge of the module. Size of the deviation of the calculated position depends on ratio of the module cell size relative to the shower size: Δ/σ (it is clearly seen on fig. 1.1). Fig. 1.2 illustrates position density structure while the modules were irradiated uniformly.

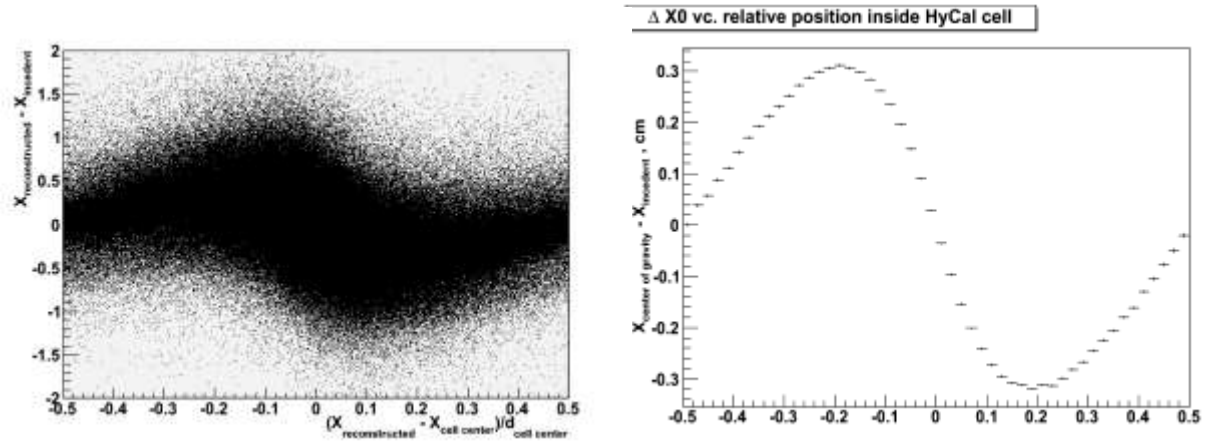

Fig. 1.1. Deviation of reconstructed coordinate from an actual value as a function of position inside a module for the center of gravity method. Left – occupancy plot, right – mean value of the deviation

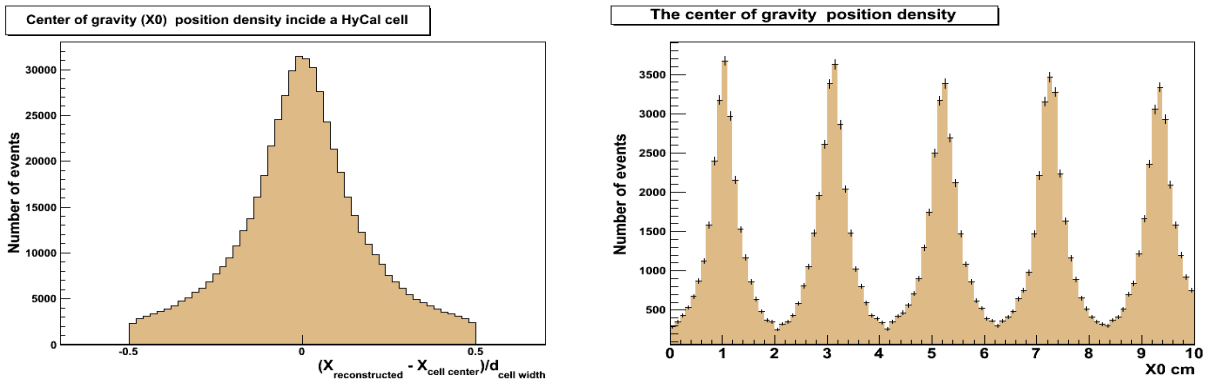

Fig. 1.2. Population of reconstructed coordinate for the simple center of gravity method: left - as a function of relative position within the crystal module: right - as a function of absolute coordinate

Since for HyCal the module size is about Moliere radius, typically only one module absorbs most of the energy and dominates in the position calculation in case when the deposited energy is weighted linearly. As the radial energy falloff of the showers is approximately exponential, there is a better way to obtain incident particle coordinates: in eq. (1.1) instead of linear weights, use the logarithmical ones:

$$w_i = max\{0, w_0 + ln(E_i / \sum E_i)\} \qquad (1.2),$$

where E_i - energy deposited in i^{th} module and w_0 is free parameter to be found. An advantage of this method is much smaller coordinate deviation from the actual value compared with linear center of gravity method. The fact that the shower radial fall off is actually a more complicated function than a single exponent is making the method biased: there are still a systematic deviation depending on impact position of the photon as fig. 1.3 demonstrates.

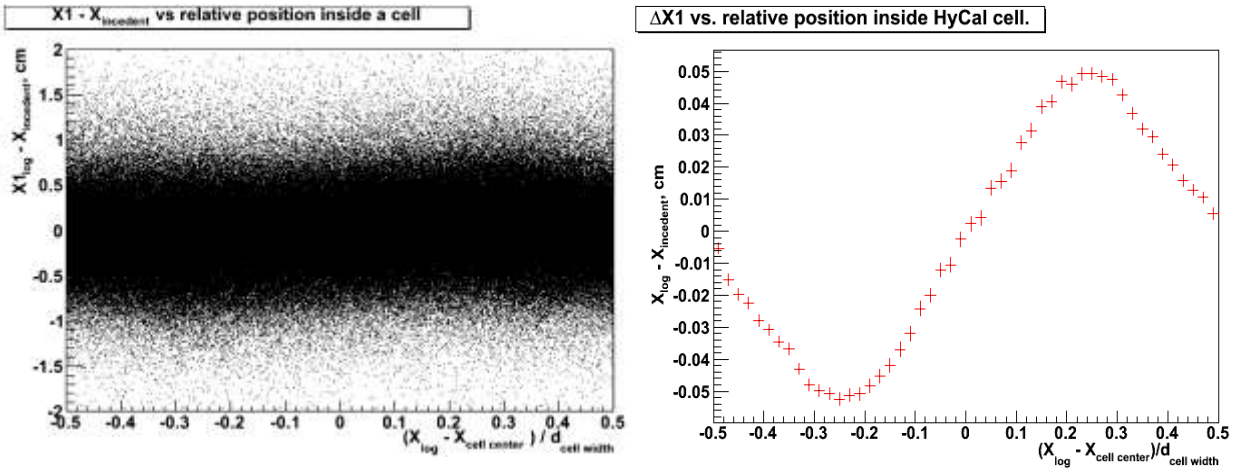

Fig. 1.3. Deviation of reconstructed coordinate from actual value as a function of relative position inside the crystal module for the logarithmic method. Left – occupancy plot, right – mean value of the deviation

Fig. 1.4 shows the structure of reconstructed population of impact points as a function of relative position within crystal module for the logarithmic method (while actual incident positions are uniformly populated). For further improvement of the reconstruction algorithm, to eliminate the most part of remaining bias affects, we apply correction function g for coordinate, reconstructed with logarithmic method:

$$x_{corrected} = x_{rec} + g(x_{rec}) \qquad (1.3).$$

The correction function was chosen as an odd order polynomial. Such a parameterization originally have been used for center of gravity method for lead glass calorimeters of GAMS and SELEX detectors [3-5]:

$$g(\xi) = (c_0 \xi + c_1 \xi^3 + c_2 \xi^5 + c_3 \xi^7)(\xi^2 - 0.25) \qquad (1.4),$$

where $\xi = (x_{rec} - x_{cell}) / d$, d – cell size, x_{rec} - reconstructed with the logarithmic method position, x_{cell} – coordinate of the nearest module center. The term of $(\xi^2 - 0.25)$ makes the value of x_{rec} unbiased at points $g = -0.5; 0; +0.5$ (i.e.at the module center and edges). We obtain parameter values: c_0 = -1.117, c_1 = - 6.634, c2 = +118.829, c3 = -390.046 with the fit procedure for PWO modules. One can see that reconstructed event population after applying such a correction is more uniform (fig. 1.5).

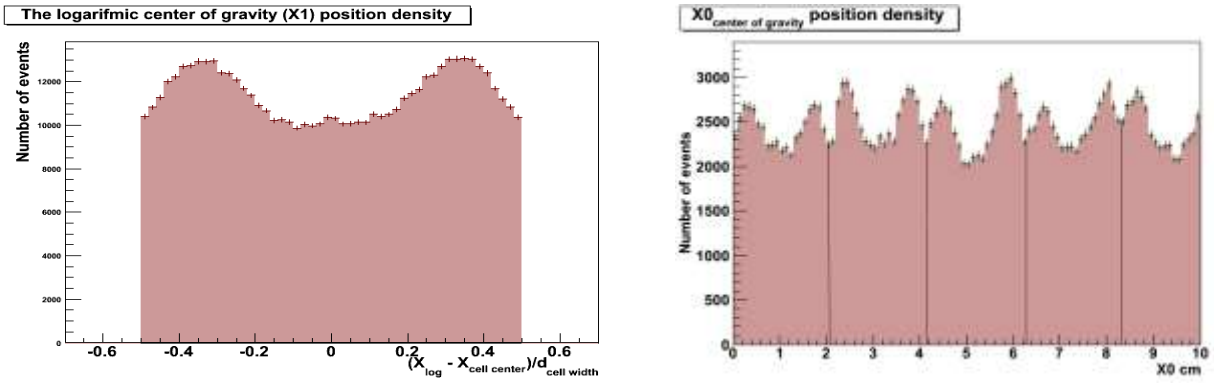

Fig. 1.4. Reconstructed hit coordinates population for logarithmic method: left – as a function of relative position within crystal module; right - as function of the absolute coordinate (module edges marked with lines)

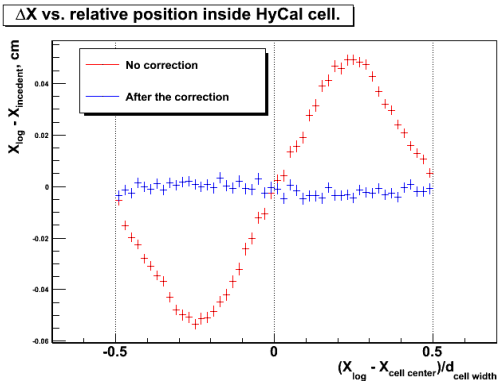

Fig. 1.5. Deviation of the reconstructed coordinate from the actual value as a function of relative position within the crystal module for the logarithmic method. Red points – no correction, blue – correction applied

After the correction, reconstructed hit point population comes quasi uniform as can be seen from fig. 1.6. Reconstructed position as a function of actual impact position is shown in fig. 1.7. To obtain such a fine calorimeter position during the snake scan we used run intervals with continuous motor motion and stable beam. We assumed the motor speed to be constant and used a high frequency clock information stored in the recorded events. The time when the beam was passing HyCal module centers was defined using biased shape of the simple center of gravity method and maximal energy deposition in the central module (see details in the next section).

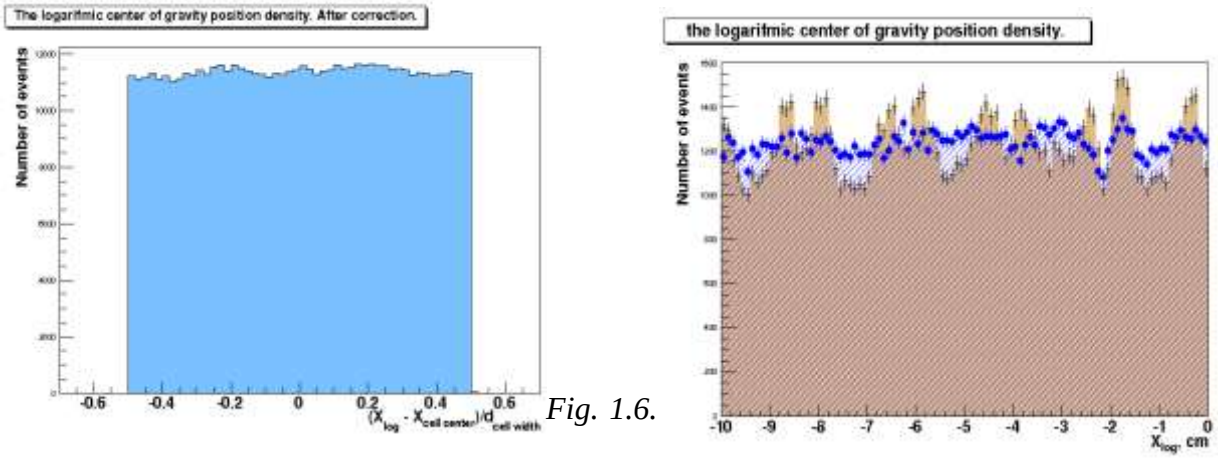

Fig. 1.6. Reconstructed with logarithmic method coordinate population: left - as function of the relative position within crystal module; right - as function of absolute coordinate: brown solid histogram - before correction, blue open histogram – after correction

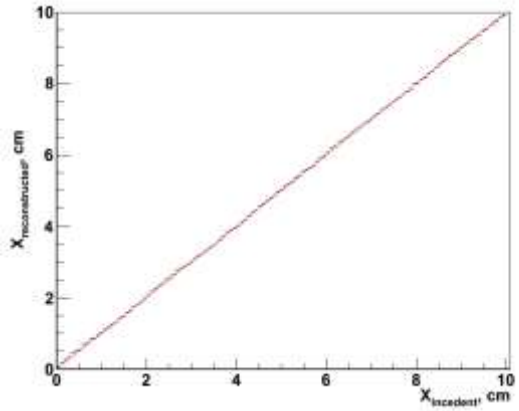

Fig. 1.7. Reconstructed position as function of actual incident position for the corrected logarithm method. Red line shows y = x curve

As we already mentioned, this correction could be applied for the center of gravity method (as it was originally done in [3-4]). For this case, we have obtained the following parameter values: $c_0 = 11.0504$, $c_1 = -92.2812$, $c_2 = 288.118$, $c_3 \equiv 0$(fixed). Fig. 1.8 shows a deviation of the reconstructed coordinate *x* from impact one as a function of relative position for the center of gravity method after correction. One can see that there is no significant bias remained, thus the population distribution (fig. 1.9) is close to be uniform.

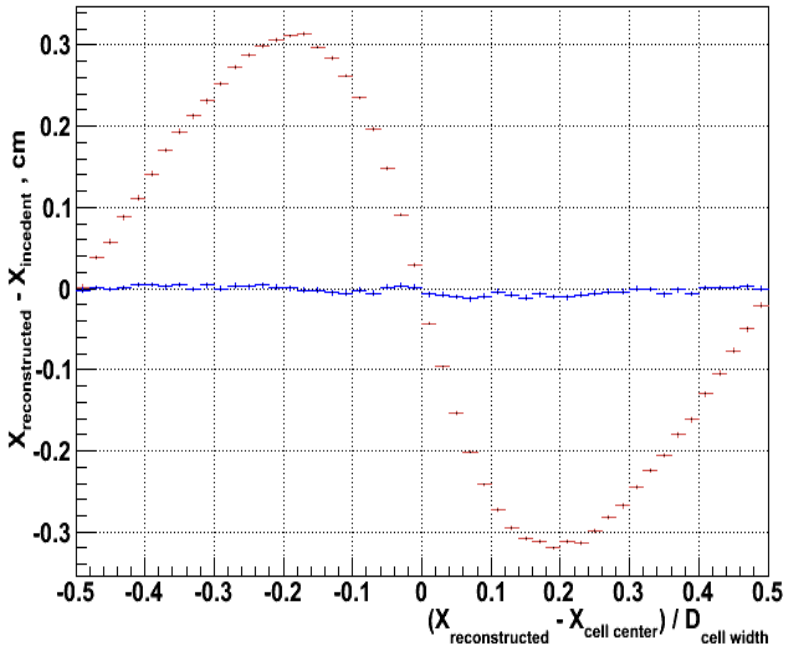

Fig. 1.8. Deviation of the reconstructed coordinate from the actual as a function of a relative position within the crystal module for the center of gravity method. Red points – before correction, blue dots – after

Several additional approaches for the correction were studied. For example, one can use a table of the deviation from the actual position to correct reconstructed coordinate. This can give better results compared to used correction function in case if such tables would be obtained for each module or at least for each small segment of the HyCal calorimeter. It is also worth to try instead of a simple logarithmic energy weighting reverse sum of two exponent functions. While simple logarithm is a reverse to exponent function, it is known that e.m. shower falls of as a sum of two exponents (so-called hard and soft cores of the profile). Hence, such a function may give a better results.

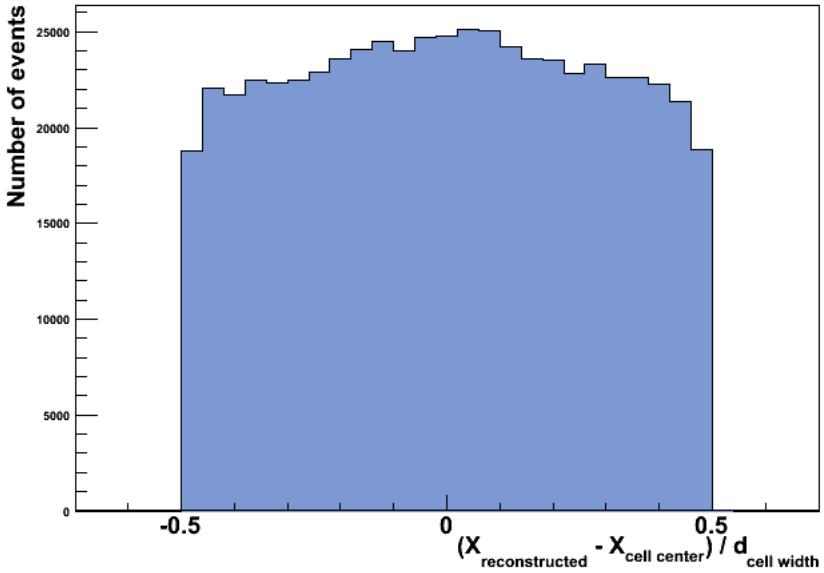

Fig. 1.9. Reconstructed hit coordinates population for the center of gravity method as a function of relative position within the crystal module after applying the correction

2. Position Resolution

To extract position resolution directly, the actual photon impact point is necessary for comparison with the reconstructed one. During the snake scan HyCal was moving horizontally along each modules raw, thus the photon beam has irradiated each module. The instantaneous calorimeter coordinate coordinate was calculated using known timing of each event (as mentioned in the previous section). This timing information has been obtained from the ALCIC quartz timer counter, which was used to control electronics dead time. For this purpose, we have selected a group of runs where the HyCal was moving with a constant speed. For crystals, we used run numbers of 5344, 5345, 5366, for lead glass – 5379. The device motion speed was found by the fitting of HyCal reconstructed coordinates.

Since the incident coordinate represents position of the photon on the HyCal face, the distribution of the difference between the reconstructed coordinate and calculated beam center position is a result of the convolution of the HyCal response and the beam spot profile. The beam spot profile was obtained separately with two methods: using a super-harp scan [6] and modeling of bremsstrahlung process in the golden

radiator by GEANT (fig. 2.1). Both methods agree within 10% accuracy. HyCal response is assumed a Gaussian distribution. Fig. 2.2 shows a distribution of the difference between reconstructed and incident positions fitted with the convolution of a Gaussian with the beam profile for 5...5.2 GeV energy. Fig. 2.3 shows position resolution as a function of energy fitted with $a/\sqrt{E}$ function. It is known from the super-harp scans that a width of the beam spot could vary by 5-10%. The effect of such variation on the obtained (unfolded) resolution is taken as our systematic uncertainty. Fig. 2.4 shows the position resolution as a function of the *x* coordinate. Red arrows indicate the borders of the modules. As very well known the worst resolution is in the center of module. It is because of energy sharing with surrounding modules (which algorithm is using for coordinate reconstruction) is minimal in this case.

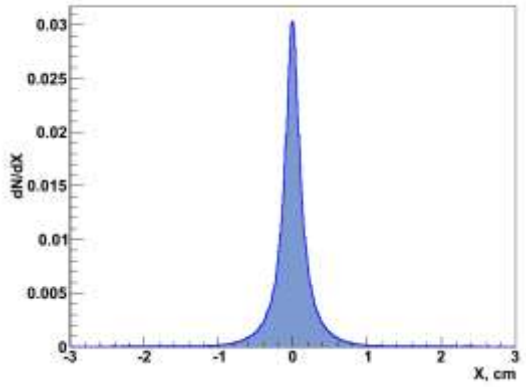

Fig. 2.1. Transverse beam profile projected onto HyCal face (GEANT model)

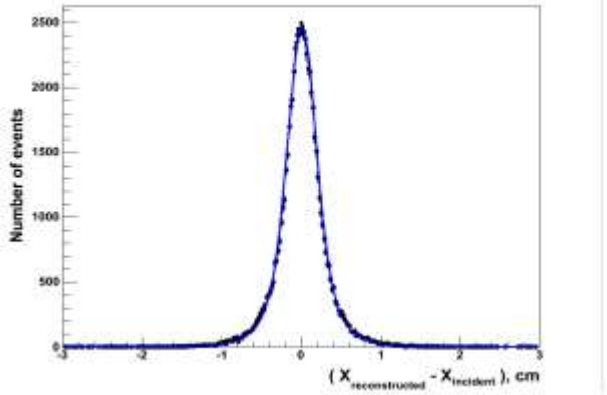

Fig. 2.2. Deviation of reconstructed coordinate from beam position fitted with the convolution of Gaussian with the beam profile

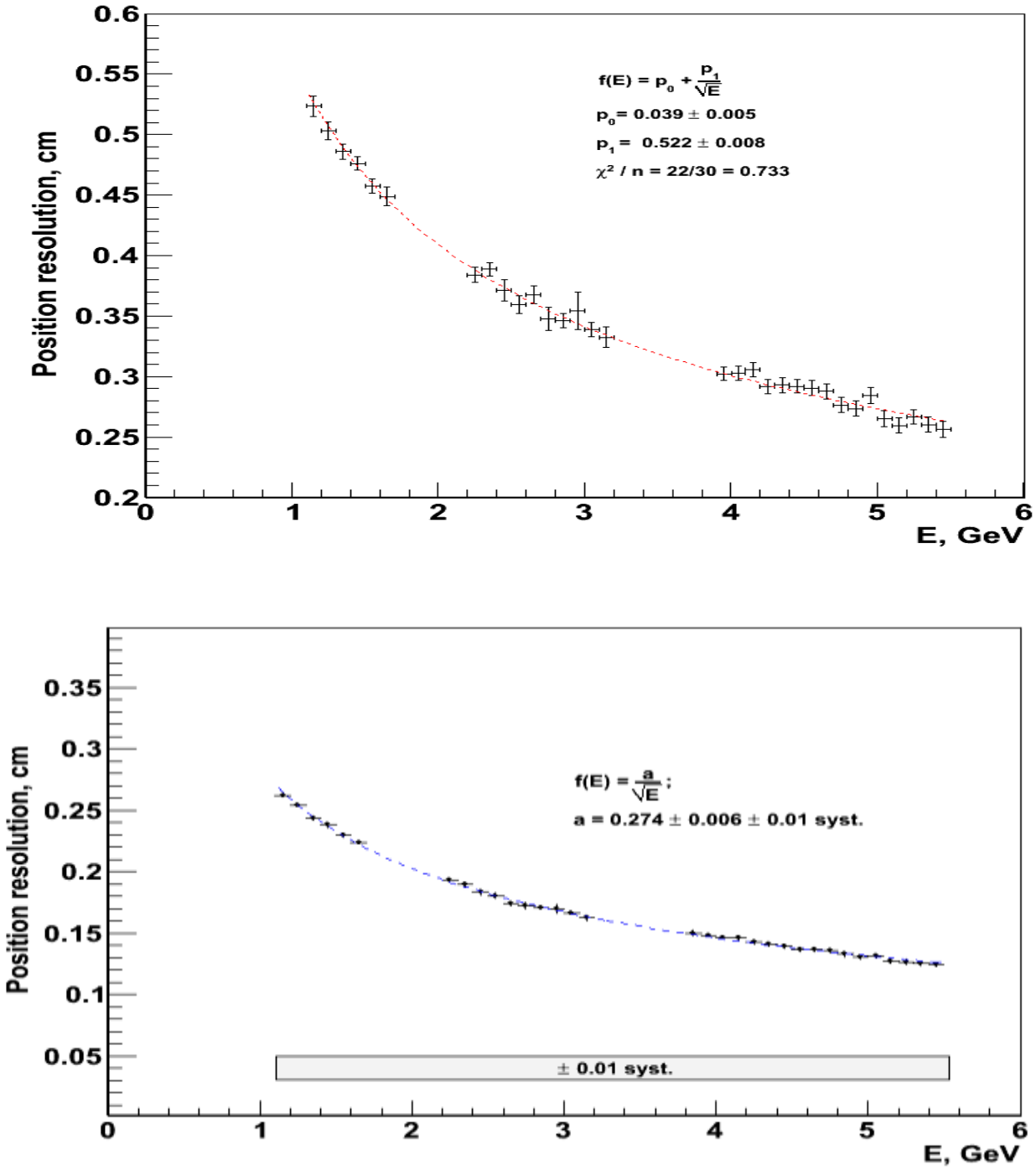

Fig. 2.3. HyCal position resolution as a function of energy: top – lead glass; bottom - PWO

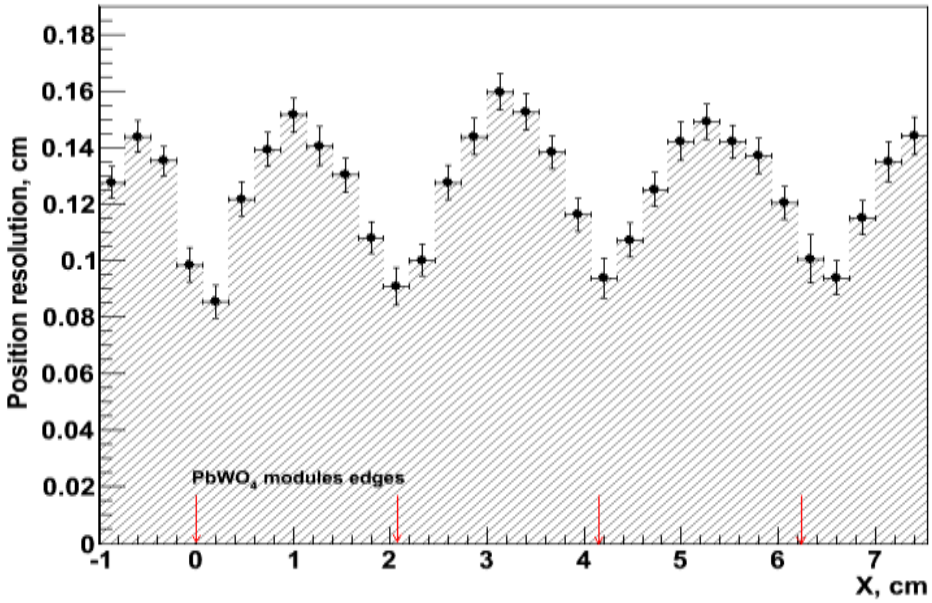

Fig. 2.4. HyCal position resolution as a function of absolute coordinate. Arrows mark module edges

3. Energy Reconstruction

Incident particle energy is estimated by sum of energy depositions in 5x5 cell cluster around the central module with the maximum energy deposition. In case if the module with maximum energy deposition is next to the transition between PWO and lead glass, all the PWO modules within the range of 2.5 PWO cell size around are included in summation. Further corrections were applied for such an energy sum as described below.

As incident photon energy is known from the tagger very well, an actual value of it at the face of the calorimeter can change due to the interactions on the way of beam. To reduce number of events with such interactions in the analysis, the fitted mean position for the last 1000 events is used to reject events, which are reconstructed at the distance more than 2 cm out of it.

Fig. 3.1 shows a ratio (mean value for many events) of energy reconstructed by HyCal and the tagger $E_{cluster}/E_{tagger}$, as a function of position within the crystal module. It clearly does not have a flat shape.

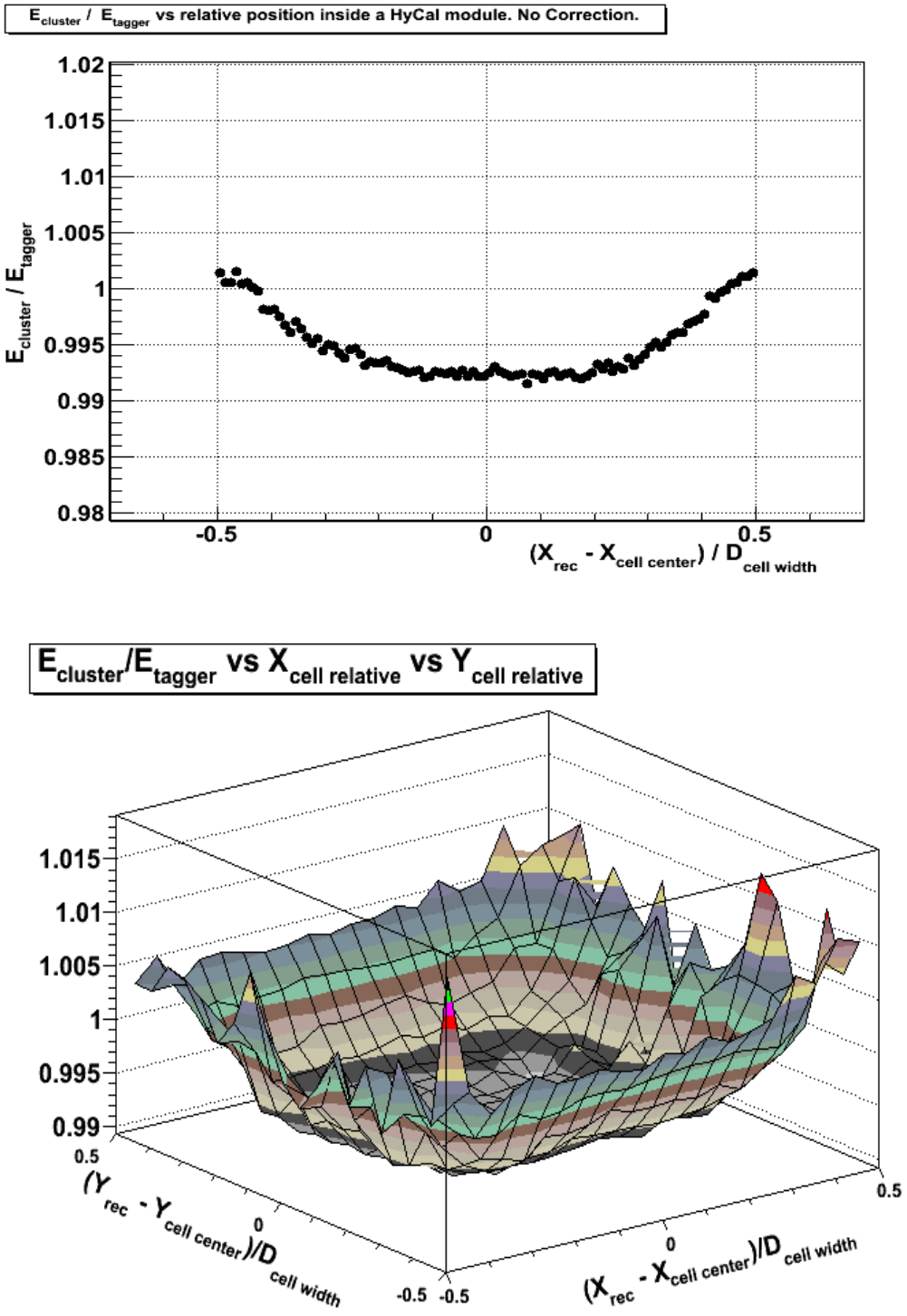

Fig. 3.1. Ratio $E_{cluster}/E_{tagger}$ as a function of hit position within calorimeter module (x-projection and 2-d plot) for PWO modules

The reason of this funny behavior is that the upstream side of HyCal module is covered by bronze flange with the half-inch diameter hole in the center. This extra surface serves as a preshower, causing a part of gammas to be converted in it and therefore shifting e.m shower position to the front. It is known [7] from beam tests, that light produced at front and end of PWO module has some (10%…20%) collection enhancement (fig 3.2).

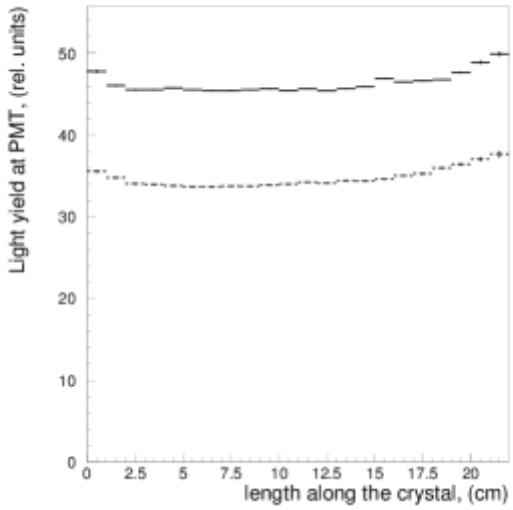

Fig 3.2 Typical light uniformity curves of PWO crystal modules obtained with transversal muon test (courtesy of Vladimir Kravtsov, IHEP Protvino)

We will correct for this effect since we know beam position during the snake scan. We will use the following correction function $f(X_{rel}, Y_{rel})$: $E = E_{reconstructed} / f(X_{rel}, Y_{rel})$, where $f(X_{rel}, Y_{rel}) = c_0 (1+ c_1 exp\{c_2 - c_3/X_{rel}^2\}) (1+ c_1 exp\{c_2 - c_3/Y_{rel}^2\})$, $X_{rel} = (X_{reconstructed} - X_{cell\ center}) / d_{cell\ width}$, $Y_{rel} = (Y_{reconstructed} - Y_{cell\ center}) / d_{cell\ hight}$. Constant values found from the fit: $c_0 = 0.99357$, $c_1 = 0.05264$, $c_2 = -0.1152$, $c_3 = 0.31194$. The ratio $E_{cluster}/E_{tagger}$ as a function of hit position within the crystal after such correction is shown on fig. 3.3. The correction slightly improves the energy resolution for high-energy part of the spectrum. It is interesting to note that for the lead glass modules, we do not have such peculiarity. This is probably because of the different light nature in lead glass.

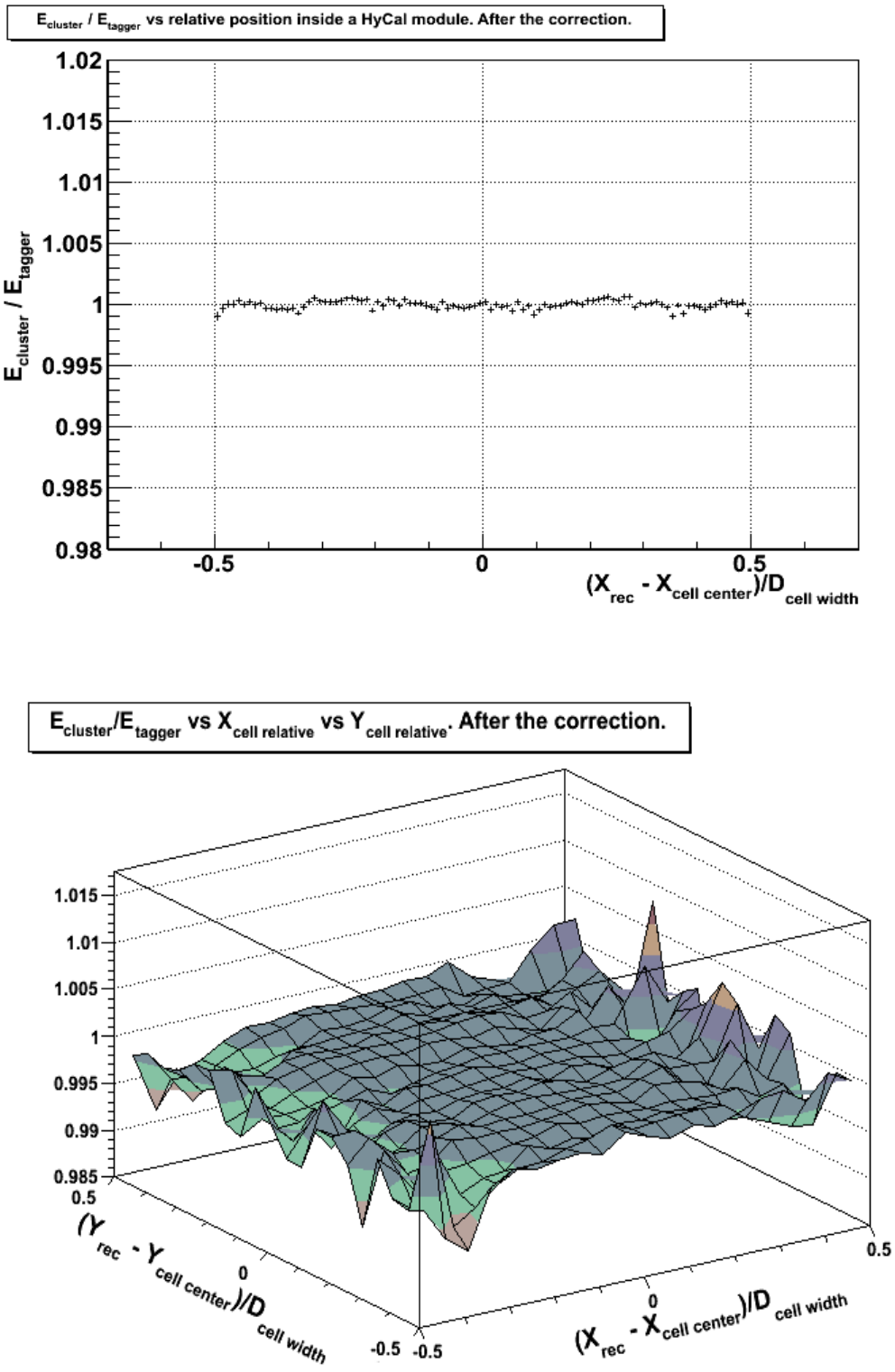

Fig. 3.3. $E_{cluster}/E_{tagger}$ ratio as a function of hit position within crystal module with correction applied (x-projection and 2-d plot)

4. Energy Resolution

To estimate energy resolution we used $E_{cluster}/E_{tagger}$ ratio distribution (Fig. 4.1).

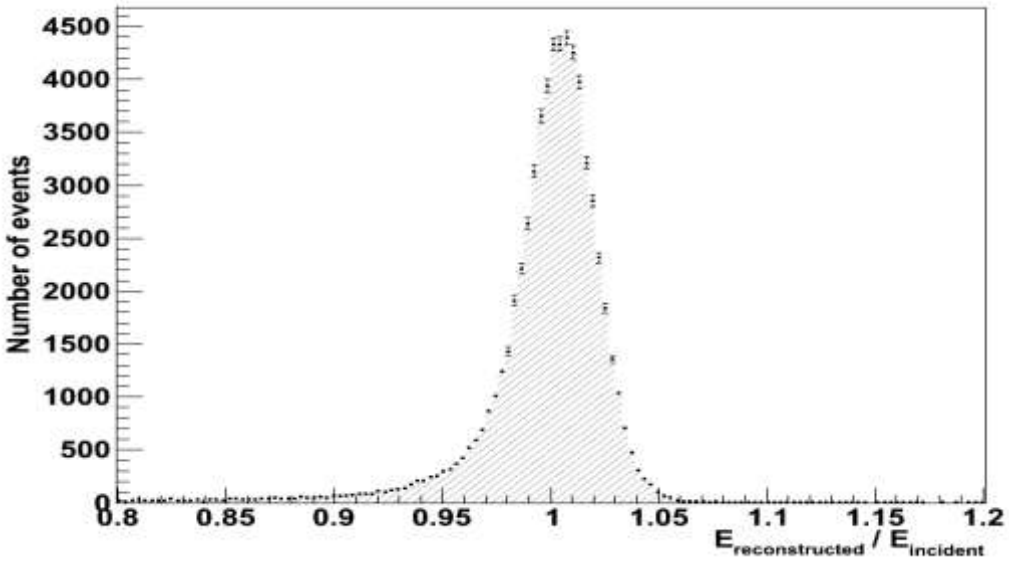

Pic 4.1 Typical $E_{cluster}/E_{tagger}$ distribution for crystals

The left tail of the distribution corresponds to energy leakage through the rear edge of the module and out of 5x5 matrix while the right tail is due to light absorption and a pile up effect. This distribution is not well described by single Gaussian distribution. There are various options to define the resolution, for example to calculate full width on the half maximum (FWHM) or to fit the distribution by sum of few Gaussians and take a weighted square sum of their width parameters. In our analysis, we used a function introduced by the Crystal Ball Collaboration (see for example [8]). We found that this function gives good agreement with the observed distribution (χ^2 of the fit is close to unit). This function, named the Crystal Ball function, is a probability distribution function commonly used to parameterize various processes with a leakage in high-energy calorimetry. It consists of a Gaussian core and a power-law low-end tail below a certain threshold. The function itself and its first derivative are both continuous.

The Crystal Ball function is defined as:

$$f(x;\alpha,n,\bar{x},\sigma) = N \cdot \begin{cases} \exp(-\frac{(x-\bar{x})^2}{2\sigma^2}), & \text{for } \frac{x-\bar{x}}{\sigma} > -\alpha \\ A \cdot (B - \frac{x-\bar{x}}{\sigma})^{-n}, & \text{for } \frac{x-\bar{x}}{\sigma} \leqslant -\alpha \end{cases}$$

where, $A = \left(\frac{n}{|\alpha|}\right)^n \cdot \exp\left(-\frac{|\alpha|^2}{2}\right), \qquad B = \frac{n}{|\alpha|} - |\alpha|\ ,$

N - normalization factor, α, *n*, *x*, <*x*>, and σ are free parameters of the fit. Examples of the Crystal Ball function shapes are given on Fig. 4.2.

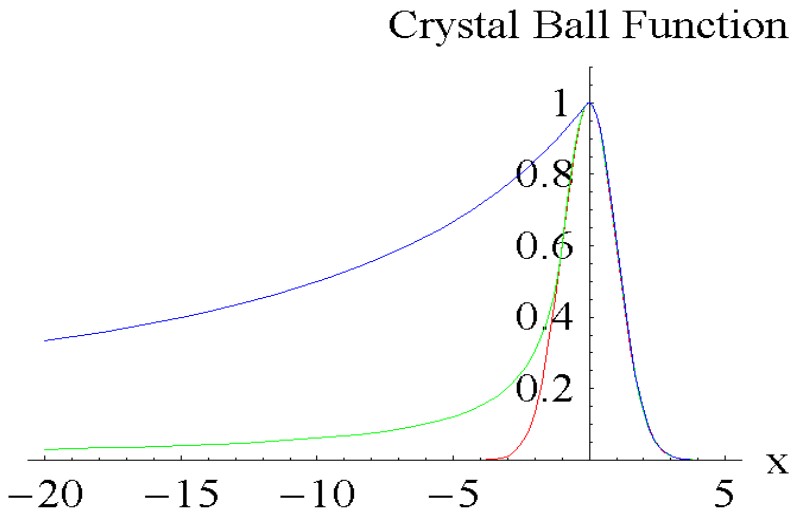

Fig. 4.2. Crystal ball function shapes for different α parameter values, and <x> = 0, σ = 1, N =1: red — α = 10; green — α = 1; and blue — α = 0.1

Fig. 4.3 shows $E_{cluster}/E_{tagger}$ distribution for PWO module fitted with the Crystal Ball function. One can see on the logarithmic scale plot (fig. 4.3(b)) that the tails are adequately described (except with a small deviation in the pile up region). Values of the resolution in the module centers and near the edges were compared. The distribution for events with an impact point within 0.5 cm distance from the cell center have significantly less size of left tail (leakage) on energy ratio plot (see fig. 4.4). The energy resolution as a function of energy for different distances from the cell center is shown in fig. 4.5. Again, one can see that the resolution for events within 0.5 cm from the cell center is better than for the edge by factor of 1.13.

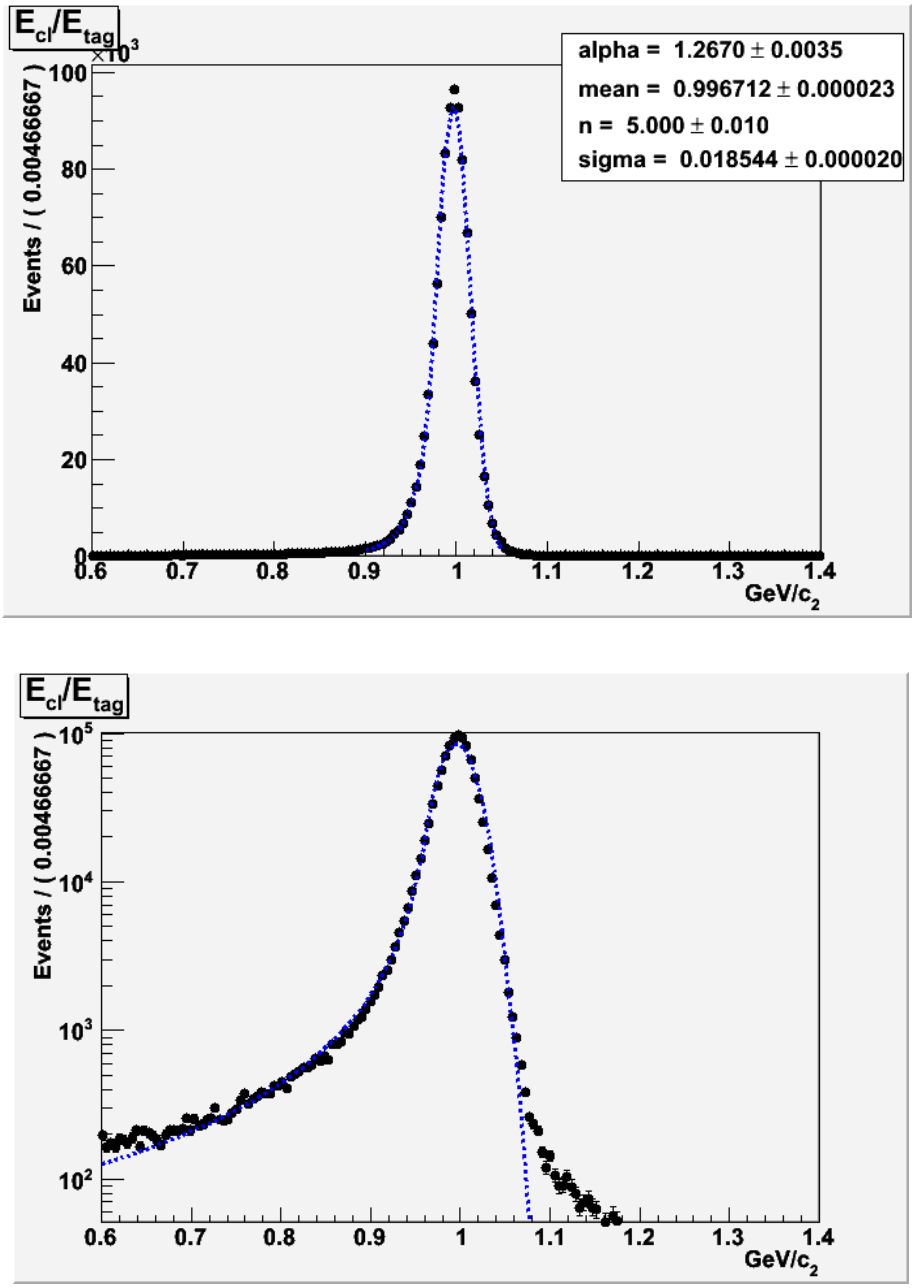

Fig. 4.3 $E_{cluster}/E_{tagger}$ ratio distribution fitted with the Crystal Ball function for E_{tagger} > 5GeV in linear and logarithmic scale (PWO modules)

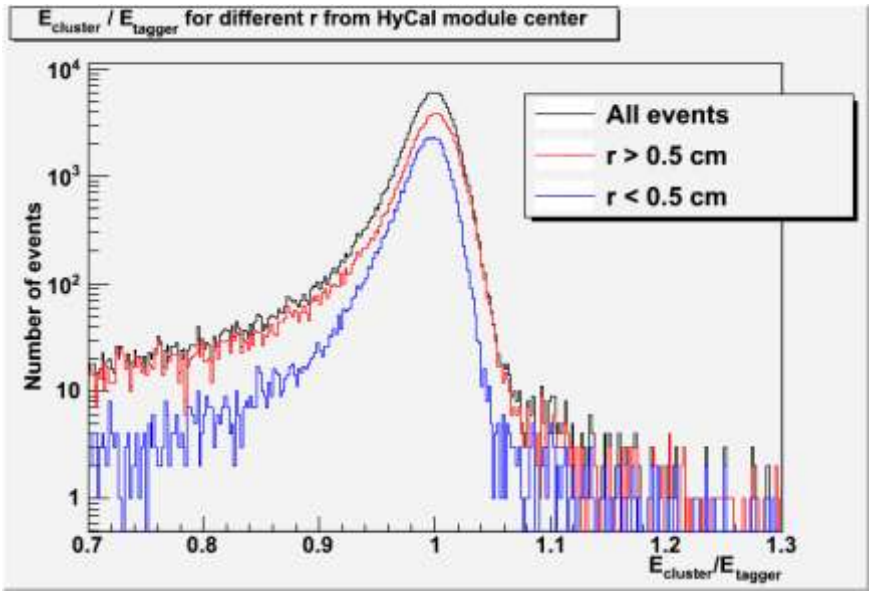

Fig. 4.4. $E_{cluster}/E_{tagger}$ distributions for inner and outer regions of the PWO module. Black histogram — all together; blue — events within r<0.5cm from the cell center; red — events outside of 0.5cm radius

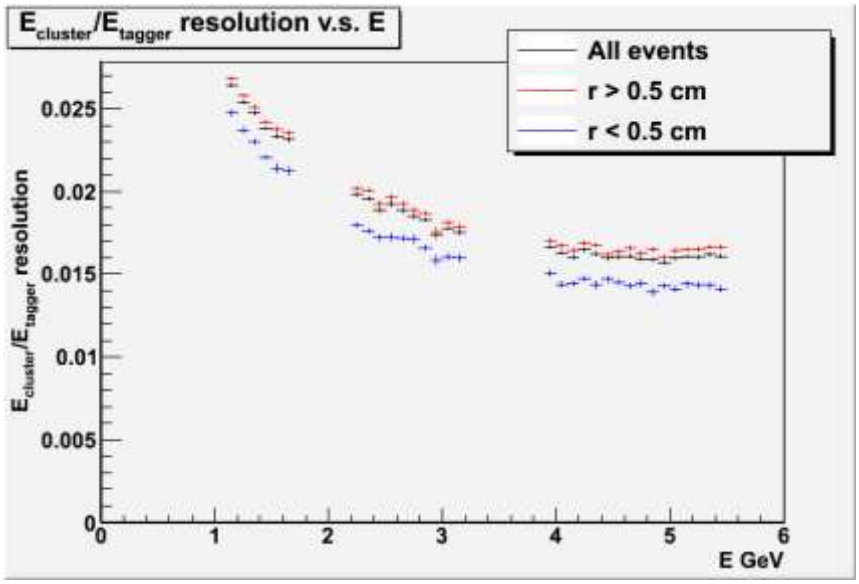

Fig. 4.5. Energy resolution as a function of energy for PWO modules. Black — all events, blue — events within r < 0.5cm from the cell center, red — events outside 0.5 cm radius

The obtained energy resolution as a function of energy for different HyCal regions is shown on fig. 4.6, 4.7; as a function of the relative position within the cell – on fig. 4.8; as a function of absolute coordinate – on fig. 4.9. The module edges resolution is getting worse due to higher leakage in between of the modules. Fig. 4.10 shows energy linearity for crystal and lead glass part of HyCal. The linearity histograms were fitted with a straight line (1st order polynomial). Reconstructed energy as a function of incident one shows good linearity.

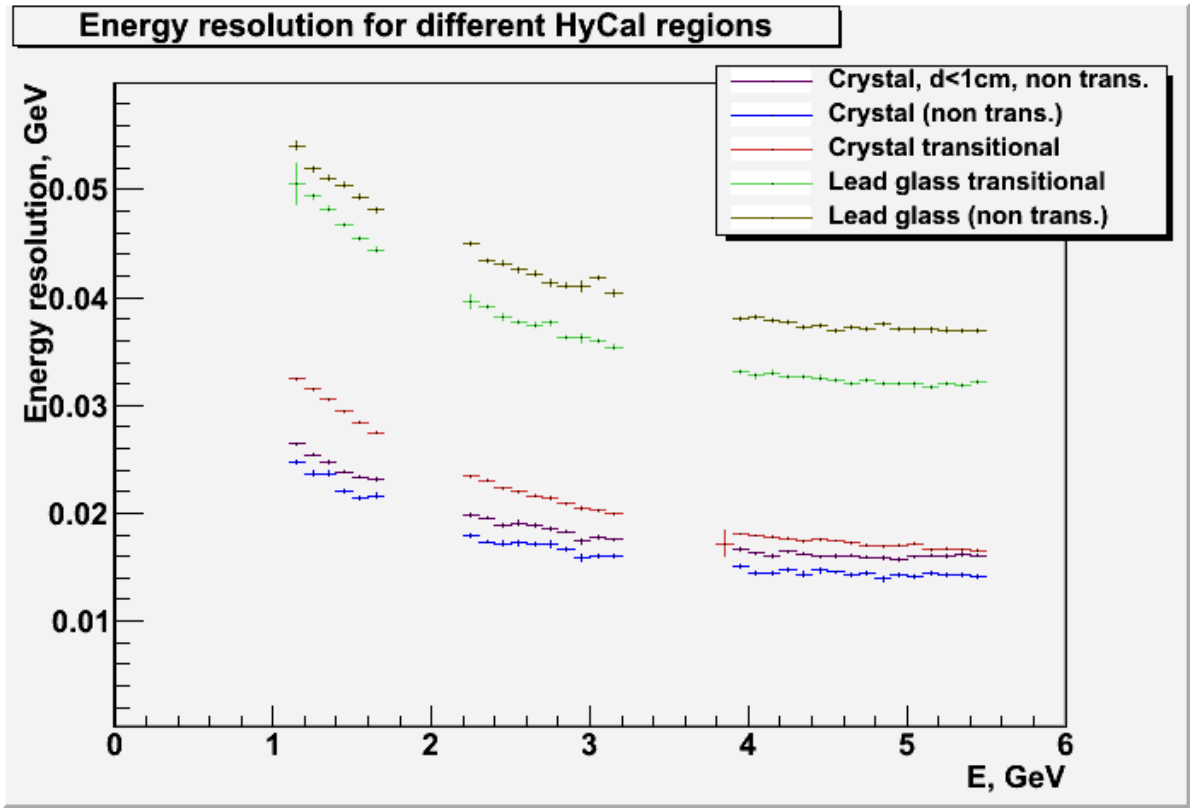

Fig. 4.6. Energy resolution as a function of energy for different HyCal regions

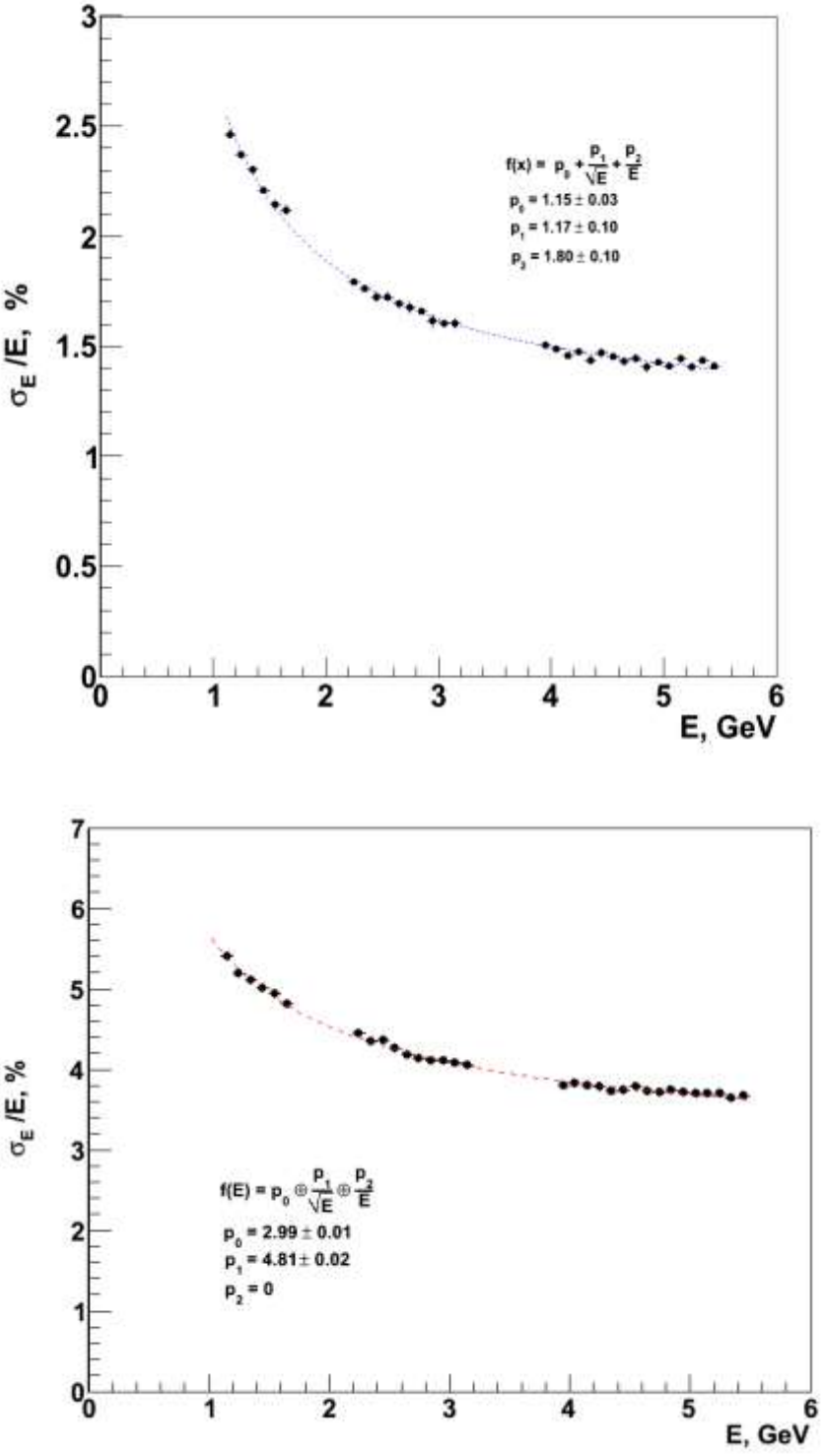

Fig. 4.7. Energy resolution as a function of energy for PWO (top) and lead glass (bottom)

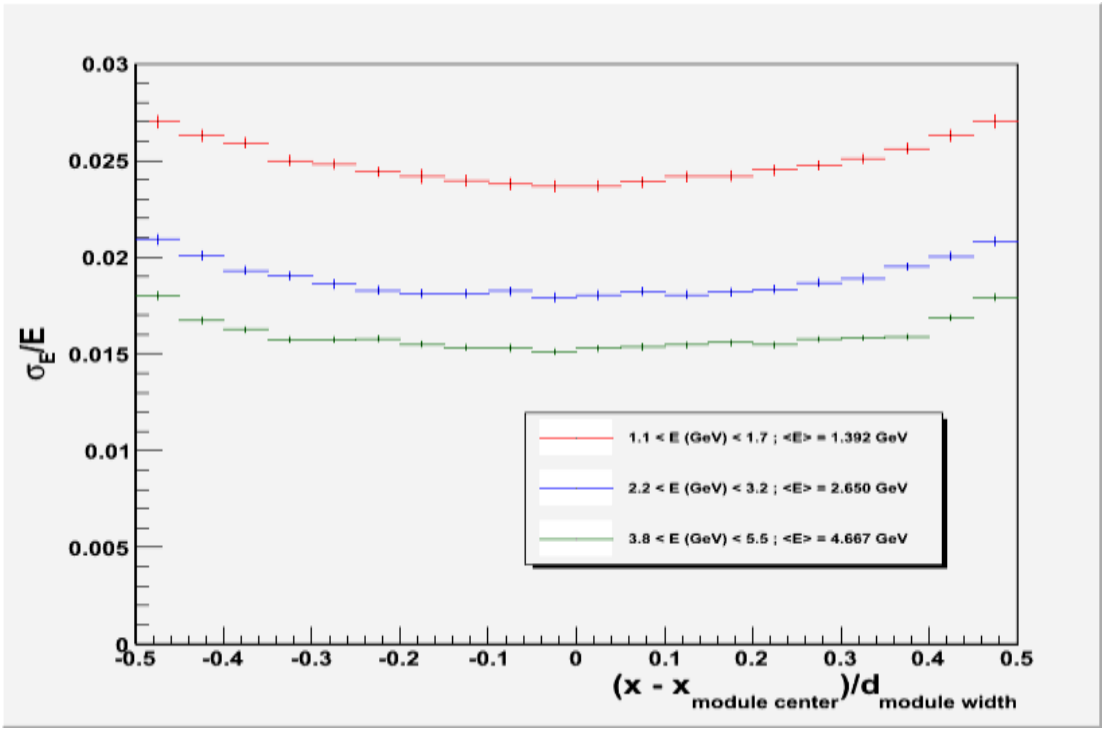

Fig. 4.8. Energy resolution as a function of relative position within crystal modules for different energy ranges

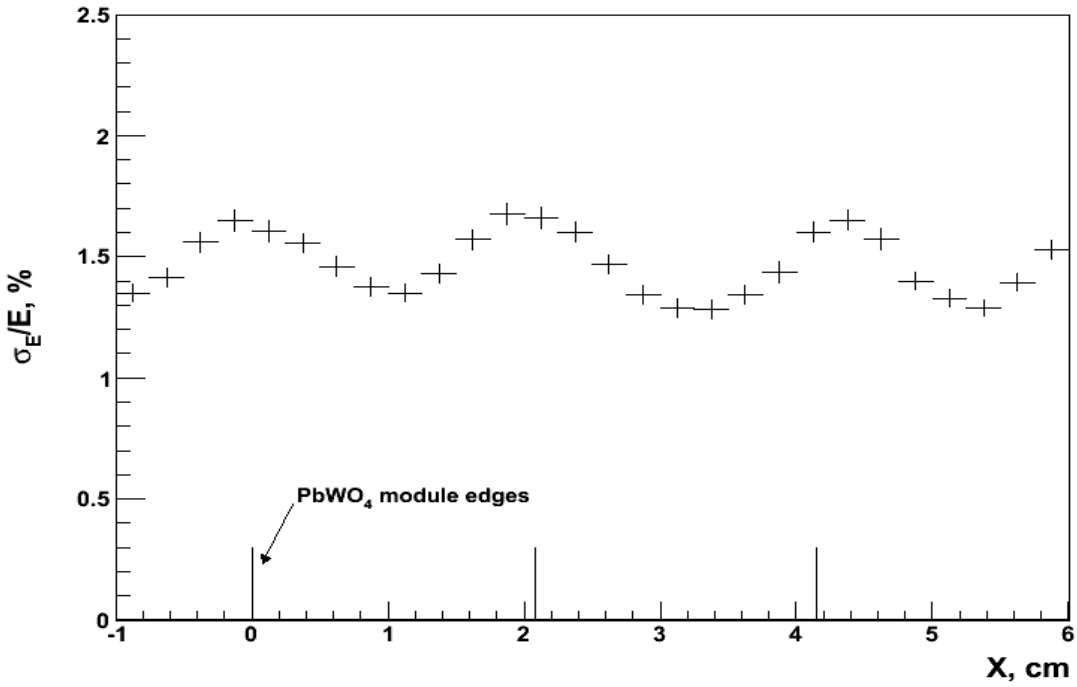

Fig. 4.9. Energy resolution as a function of absolute coordinate for 4.0...5.5GeV for PWO crystals. Lines mark module borders

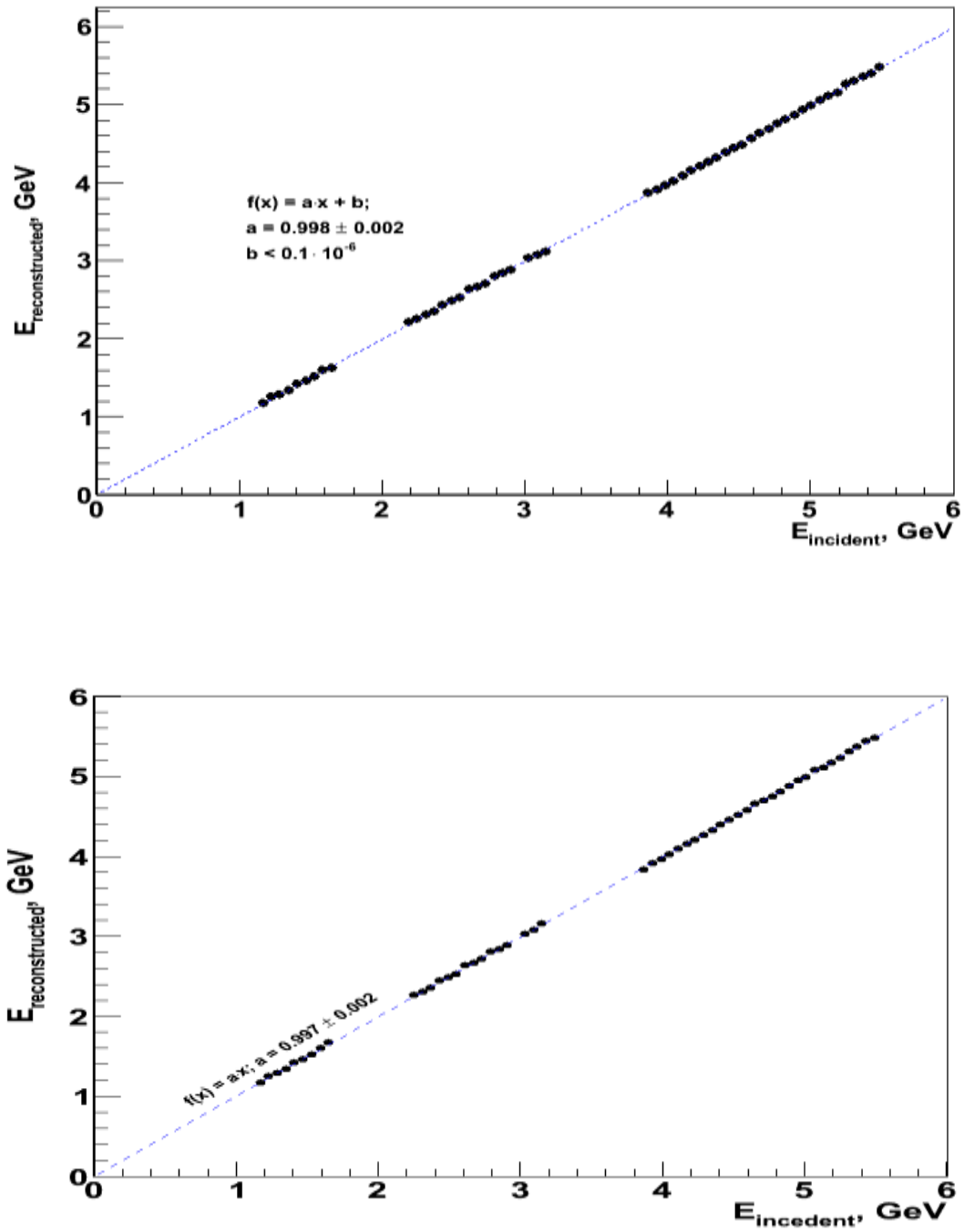

Fig. 4.10. Observed energy linearity: top — crystals; bottom — lead glass

5. PWO Crystal — Lead Glass HyCal Transition Region

To study spatial and energy resolution behavior in the transition area between PWO and lead glass, we used data from special fixed HyCal position runs 4245- 4266. In these runs, beam position vs HyCal has been fixed. The shift value from the center of W1086 module has been changed by the given preselected values (see fig. 5.1). Beam profile shape (fig. 2.1) have been taken into account in extraction of the spatial resolution. Fig. 5.2, 5.3 show spatial and energy resolution as a function of absolute coordinate $X_{incident}$ for 5.0...5.5GeV photon beam energy. Both resolutions increase while approaching transition line because of the fact that more and more lead glass material and less PWO crystals are involved. Fig. 5.4 shows ***X***-coordinate reconstructed as function of incident photon coordinate ***x***. Function ***f(x) = x*** was added for comparison. Reconstructed position deviation near the transition line are presumably due to the leakage caused by protrusion of the lead glass modules face plane over the PWO modules face plane. It is likely that the same leakage effect is responsible for underestimation of reconstructed energy that can be seen on fig. 5.5. Possible corrections for this leakage effect in the transition region would be highly angular dependent and cannot be transferred from the snake scan physics data.

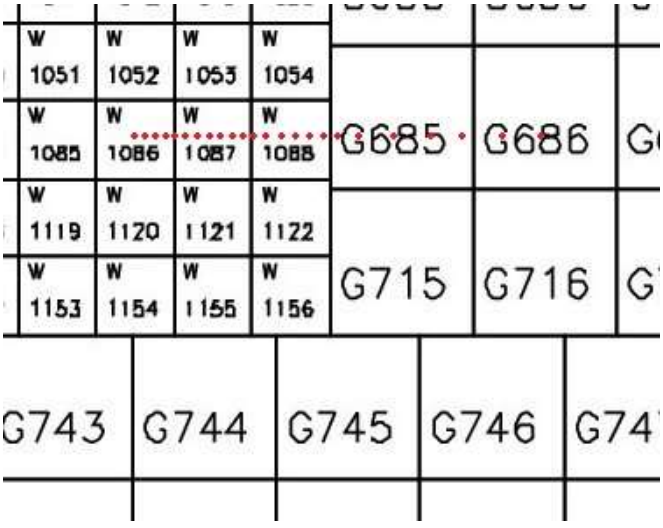

Fig. 5.1. The HyCal map fragment with the fixed beam positions marked by red dots

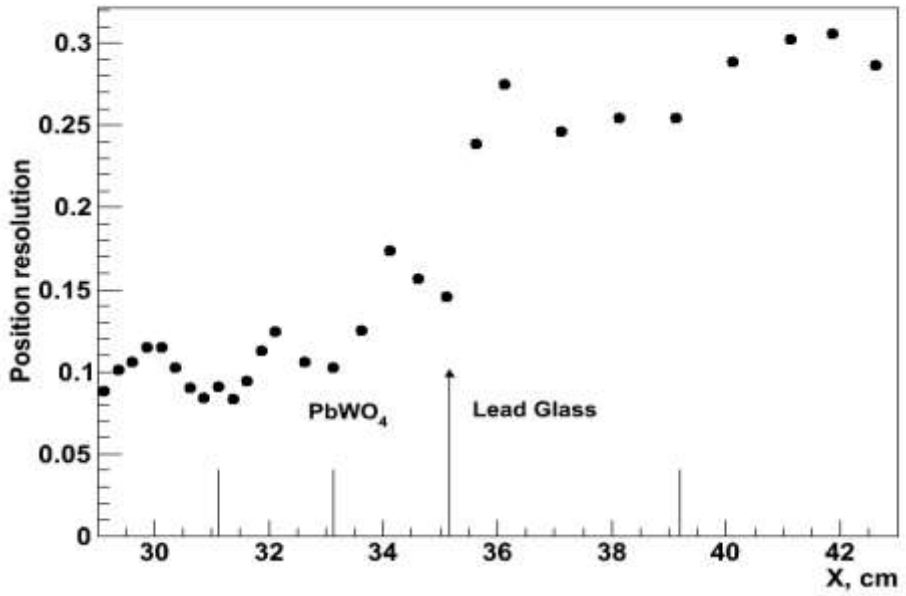

Fig. 5.2. Position resolution as function of absolute coordinate $X_{incident}$ for 5.0...5.5GeV. Lines show cell borders, arrow shows transition line

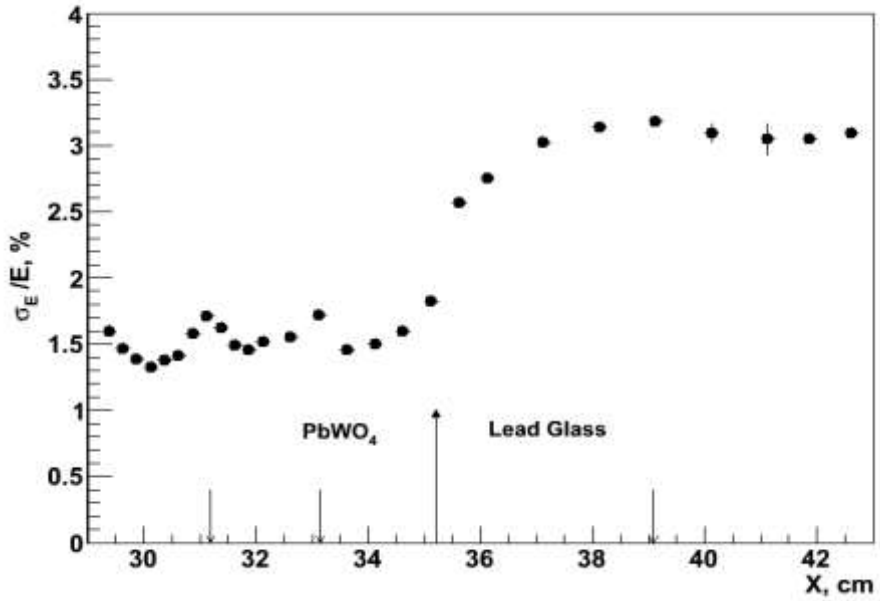

Fig. 5.3. Energy resolution as a function of absolute coordinate $X_{incident}$ for 5.0...5.5GeV. Lines show cell borders, arrow shows transition line

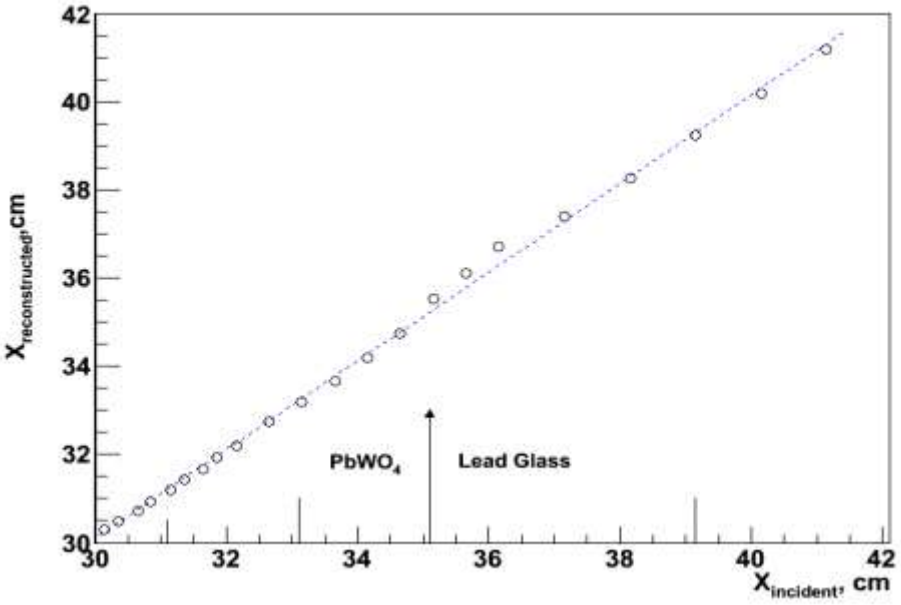

Fig. 5.4. $X_{reconstructed}$ as a function of $X_{incident}$ for 5.0...5.5GeV photon beam energy

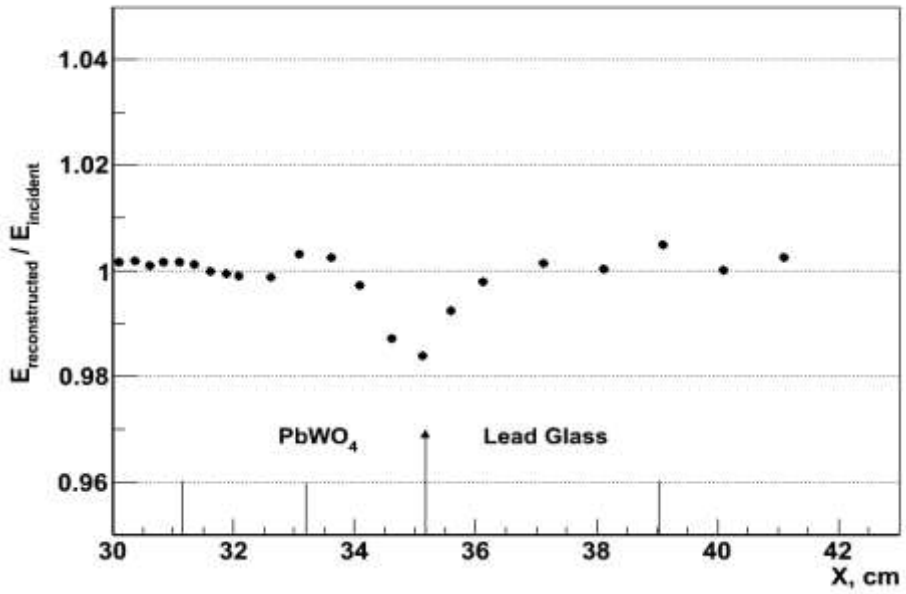

Fig. 5.5. $E_{reconstructed}$ / $E_{incident}$ mean value as a function of an absolute x coordinate for 5.0...5.5 GeV photon beam energy

Conclusion

1. Data from the first and second snake scans were used for energy and coordinate resolution analysis and HyCal calibration
2. New module calibration coefficients were obtained and stored in PrimEx database with "*gain5_iter*" attribute for the PWO and lead glass modules
3. A method to restore beam impact horizontal coordinate from timing information was developed and successfully implemented
4. HyCal position reconstruction was revisited. Additional fine corrections for the center of gravity and logarithmic methods were found and applied. These fine corrections to the position reconstruction algorithms were added to *prim_ana* analysis program. The PrimEx source version control system has been updated
5. Energy reconstruction was revisited. Fine correction for energy reconstruction in crystal modules were designed. This fine correction algorithm was added to *prim_ana*. PrimEx source version control system has been updated
6. Position reconstruction resolution and linearity were studied. Obtained values for resolution at 5.4...5.5GeV gamma energies are: 0.12cm ± 0.01cm for crystals and 0.26cm ± 0.01cm for lead glass
7. Energy resolution and linearity were studied. Obtained resolution values for 5.4...5.5GeV gamma energies are: 1.41% ± 0.02% for crystal modules and 3.61% ± 0.05% for lead glass modules
8. Position and energy resolutions and linearity for the PWO-lead glass transition region were studied

References

1) “Performance of PrimEx Electromagnetic Calorimeter”, M. Kubantsev, A. Gasparian, I. Larin, CALOR 2006 Proceedings, Vol. 867, Chicago: AIP Conf. Proc.: 2006, P. 51

2) “Precision measurement of the neutral pion lifetime based on the Primakoff method”, I. Larin Ph.D. Thesis (in Russian) https://userweb.jlab.org/~ilarin/thesis/thesis_ilarin.pdf

3) “Separation of the overlapping electromagnetic showers in the cellular GAMS type calorimeters”, A.A. Lednev (Serpukhov, IHEP), Dec 1993. IFVE-93-153

4) “Electron shower transverse profile measurement”, A.A. Lednev , NIM A 366 (1995)

5) “The lead - glass electromagnetic calorimeter for the SELEX experiment”, M.Y. Balatz et al., Nucl.Instrum.Meth. A545 (2005) 114-138

6) P. Ambrozewicz, PrimEx Note #43, “Beam Quality Study”, March 9, 2007

7) Vladimir Kravtsov, IHEP, Protvino, private communications

8) https://en.wikipedia.org/wiki/Crystal_Ball_function